# TITLE

**Composition of a spatial engram in mouse dentate gyrus**


**AUTHORS**

*Wilmerding, Lucius K.[1,2,3], Kondratyev, Ivan[1], Ramirez, Steve[1,2,3], Hasselmo, Michael E.[1,2,3]

**AFFILIATIONS**

[1]Center for Systems Neuroscience, Boston University

[2]Graduate Program for Neuroscience, Boston University

[3]Department of Psychological and Brain Sciences, Boston University

* Corresponding Author: lwilmerd@bu.edu


**Highlights**

- Immediate-early-gene labeling strategy revealed spatial navigation ensembles in DG
- Both novelty and memory demand contribute to recruited ensemble size
- Sub-ensembles encode separate maze routes within a larger task context


**SUMMARY**

The dentate gyrus (DG) of hippocampus is hypothesized to act as a pattern separator that distinguishes between similar input patterns during memory formation and retrieval. Sparse ensembles of DG cells associated with learning and memory, i.e. engrams, have been labeled and manipulated to recall novel context memories. Functional studies of DG cell activity have demonstrated the spatial specificity and stability of DG cells during navigation. To reconcile how the DG contributes to separating global context as well as individual navigational routes, we trained mice to perform a delayed-non-match-to-position (DNMP) T-maze task and tagged DG neurons during performance of this task on a novel T-maze. The following day, mice navigated a second environment: the same T-maze, the same T-maze with one route permanently blocked but still visible, or a novel open field. First, we found that novelty and memory demand yielded larger engram ensemble size. Additionally, the degree of engram reactivation across days differed based on the traversal of maze routes, such that mice traversing only one arm had higher overlap than chance but less overlap than mice running the full two-route task. These differences could not be fully explained by behavioral differences across groups on the second day. Together, these results support the hypothesis that DG contributes to spatial navigation memory and that partially non-overlapping ensembles encode different routes within the context of different environments.

**Keywords**
Hippocampus, Engram, Immediate Early Gene, Delayed Non-Match to Position, Context, Memory, Spatial Navigation

# 1. INTRODUCTION

The dentate gyrus (DG), a subregion of the hippocampal formation, is hypothesized to act as a pattern separator that distinguishes between similar input patterns during memory formation and retrieval (Marr, 1971; McNaughton & Morris, 1987; O'Reilly & McClelland, 1994; Treves & Rolls, 1994; Hasselmo & Wyble, 1997; Leutgeb et al., 2007; Neunuebel & Knierim, 2014). Sparse ensembles of DG memory-associated granule cells, or engram cells, have been optogenetically targeted to successfully influence memory-associated behavior (Liu et al., 2012; Ramirez et al., 2013; Denny et al., 2014; Redondo et al., 2014) even after consolidation (Kitamura et al., 2017) and pathogenic aging leading to natural recall failure (Roy et al., 2016). These findings support the hypothesis that the DG encodes the contextual dimension of memories. Another body of literature emphasizes the spatial representations of DG granule cells, which exhibit place fields similar to those in CA1 (O'Keefe & Dostrovsky, 1971; Neunuebel & Knierim, 2012, 2014; GoodSmith et al., 2017; Hainmueller & Bartos, 2018; Cholvin et al., 2021). Lesions of the DG granule cell population impair spatial memory (McLamb et al., 1988; McNaughton et al., 1989; Nanry et al., 1989; Xavier et al., 1999; for a review, see Xavier & Costa, 2009) and reduce both spatial specificity of CA3 place cells and reward-associated sharp-wave-ripple rate (Sasaki et al., 2018). Reconciling how the DG contributes to both novel contextual learning and spatial representations would offer important insight into the contribution of this region for learning and memory.

To that end, our study investigated the role of the DG in distinguishing between multiple routes within a single T-maze context during a spatial navigation task. Male and female mice were trained on a delayed-non-match-to-position (DNMP) task with two routes. A population of active DG granule cells was visualized using an immediate-early-gene strategy of labeling c-Fos positive cells active during exposure on Day 1 to a novel 2-route T-maze (Guzowski et al., 1999; Reijmers et al., 2007; Liu et al., 2012; Ramirez et al., 2013). Another population of c-Fos positive cells activated on Day 2 by a second behavioral context was visualized with immunohistochemical staining for comparison. We hypothesized that the DG of mice exposed to a 1-route maze on Day 2 would show more overlap between the two cell populations than chance, but less overlap than mice re-exposed to the full 2-route maze from Day 1. Our findings support this hypothesis and additionally reveal an effect of both novelty and task demand on the size of a recruited spatial engram ensemble. Our results indicate that the DG plays an active role in encoding particular sub-routes of a 2D environment during ongoing spatial behavior.

# 2. METHODS

## 2.1 Subjects

18 wildtype (WT) C57B6J male and female mice (Jax) were segregated by sex and group-housed prior to surgery. They received food and water ad libitum and were placed on a diet containing 40 mg/kg doxycycline (dox; Bio-Serv) at least 1 week prior to surgery at the age of 17-36 weeks. Post-surgically, the mice were housed in pairs (by sex) on a reverse 12 hour light-dark cycle. Mice were split equally into groups using random assignment, counterbalancing for sex. All procedures related to mouse care and treatment were in accordance with Boston University and National Institutes of Health guidelines for the Care and Use of Laboratory animals.

## 2.2 Viral constructs and packaging

The AAV-cFos-tTA and AAV-cFos-tTa-TRE-eYFP were constructed as described previously (Ramirez et al., 2013) and sourced from Gene Therapy Center and Vector Core at the University of Massachusetts Medical School. The viral titrations were $1.5*10^{13}$ genome copy per mL for AAV-cFos-tTA-TRE-eYFP and $1.5*10^{13}$ genome copy per mL for AAV-cFos-tTA.

## 2.3 Stereotactic injection

All surgeries were performed under stereotactic guidance and all coordinates are reported relative to bregma. Anesthesia was induced with 5.0% isoflurane and maintained thereafter at a concentration of 1.5-2.0%. Bilateral burr holes were made at -2.2 mm (AP) and +/-1.3 (ML) using a 0.5mm drill to allow a 10uL nanofil syringe (World Precision Instruments) to be lowered to 2.0 mm (DV). 300nL of AAV virus cocktail was injected bilaterally at a rate of 100nL/min controlled by a MicroSyringe Pump Controller (World Precision Instruments). Following injection, the needle was kept at the injection site for 5 minutes and slowly withdrawn afterwards. Bone wax was gently inserted into the burr holes to seal the skull, and two to three sterile sutures were used to close the wound. Post-operative subcutaneous injections of Buprenorphine (0.1 mg/kg) and Ketoprofen (5 mg/kg) were administered for three days following surgery and Enrofloxacin (10 mg/kg) for five days post-surgically.

## 2.4 Behavioral assays and engram tagging

All behavioral assays were performed during the light cycle of the day (7:00 - 18:00) on animals 17-32 weeks old. Mice were handled 2-5 min per day for two days before behavioral training. To increase training motivation, mice were water restricted during the training period, tagging and re-exposure period to 20 minutes of *ad libitum* water access daily, in addition to sucrose consumed in the maze.

Behavior was run in a two-arm T-maze, as previously described (Fig. 1; Levy et al., 2021). The paradigm consisted of a sampling phase and a testing phase, separated by a 15-second delay period in a closed-off start box. During the sampling phase, mice

were forced to run a particular arm of the maze by the application of a barrier closing off the other reward arm. In the following test phase, mice were allowed to choose either arm and reward was only delivered for choosing the opposing arm to the preceding sample phase. Each mouse received five, 15-minute sessions of pre-training on the DNMP paradigm with gradually increasing delay in the week prior to surgery. Five additional training sessions of the same length, with full 15-second delay, were delivered after surgical recovery. All of these initial training sessions were carried out in the training maze, Context T: a grey, wooden, rectangular T-maze (66 cm long x 31 cm wide x 19 cm high), with opaque walls forming the central stem and different wall cues on each reward arm.

During the tagging window, mice were taken off dox for 48 hours and subsequently performed the DNMP paradigm in a novel T-maze, referred to as Context A: a beige, triangular, linoleum-lined T-maze (78 cm long x 78 cm wide x 18 cm high) with novel cue cards on the walls of the reward arms. The maze location, odor and floor texture were also changed relative to Context T. Context A had no walls on the stem, allowing mice to see the entire arena even when reward arm barriers were present. All mice were exposed to Context A for 20 minutes, with a minimum of ten DNMP trials performed. Immediately after tagging, the mice were placed back on dox for the remainder of the study. The following day, mice were pseudo-randomly split into three groups, counterbalancing for sex. The first group ran the full T-maze in Context A under the DNMP paradigm discussed above, for 20 minutes. The second group ran a one-sided route inside the maze (either left side only or right side only), with the other arm being blocked with opaque barriers, for 20 minutes (Context B). The mice in this group were evenly split between the two Half-T routes via pseudorandom assignment and were counterbalanced by sex. The third group was placed in a novel Open Field context C: an empty, opaque gray box (41.5 cm long x 39.5 cm wide x 28.5 cm high) with no top. These mice explored context C for 20 minutes without water reward.

Deeplabcut (Mathis et al., 2018) was used to extract mouse position during behavioral trials from 50fps video recorded on an overhead Mako G-131c GigE camera (Allied Vision). Video timestamps, spatially scaled position, distance, and velocity information were extracted using the CMBHome framework (https://github.com/hasselmonians/CMBHOME/wiki).

## 2.5 Immunohistochemistry.

Mice were euthanized by administration of Euthasol (390 mg/kg) and anesthetized with Isoflurane prior to transcardial perfusion with saline and 10% formalin. Extracted brains were kept in formalin for 1-7 days at 4 ℃ and transferred to 30% sucrose solution for approximately three days at 4 ℃ to undergo cryoprotection. Brains were sliced using a cryostat into 50μm slices, and blocked for 2 hours at 4 ℃ in 1x phosphate-buffered-saline + 2% Triton (PBS-T) and 5% normal goat serum (NGS). Slices were incubated for

48 hours at 4 ℃ with primary antibodies diluted in 5% NGS in PBS-T as follows: rabbit anti-cFos (1:1000, Abcam, #190289) and chicken anti-GFP (1:1000, ThermoFisher, #A10262). Subsequently, the slices were washed three times for 10 minutes in PBS-T, followed by a 2 hour incubation in the secondary antibodies diluted in 5% NGS in PBS-T as follows: Alexa 555 goat anti-rabbit (1:200; ThermoFihser, #A21429) and Alexa 488 goat anti-chicken (1:200, ThermoFisher, #A11039). Finally, the slices were mounted on slides using VECTASHIELD® Hardset™ Antifade Mounting Medium with DAPI (Vector Labs, #H-1500) and sealed with nail polish.

## 2.6 Image Acquisition

Images were acquired with an FV10i confocal laser-scanning microscope, using 60x magnification / 1.4 NA oil-immersion objective. For each image, three z-slices, separated by approximately 19.5μm, were acquired. The first z-slice was positioned at the lowest in-focus portion of the sample, the second was positioned at the center of the sample and the first was positioned at the highest in-focus portion of the imaged sample. The depth between the slices has been adjusted accordingly to ensure this composition, but was never set below 17 μm to minimize the potential of imaging the same cell in different z-planes. Before acquiring each image, the intensity of each channel (R, G, B) was configured to be approximately equivalent between all slices. Each image was acquired as a series of 1024x1024 pixel tiles which were subsequently stitched together to produce the final image (https://imagej.net/plugins/image-stitching). The images used 16 bit-depth encoding and all image processing was handled in ImageJ / FIJI (https://imagej.nih.gov/ij/) with the Bioformats toolbox (https://imagej.net/formats/bio-formats).

## 2.7 Cell Counting

Image acquisition was performed only on slices with successful targeting to the dorsal DG. cFos+ and eYFP+ cells in the upper and lower DG blades were counted using five 50um coronal slices of dorsal DG in each animal. Three z-planes were taken at a minimum 17um apart in each slice, and the cell counts from each z-plane summed for that slice. For each slice, a region of interest was defined by an experimenter blind to the identity of the image but not the nature of the experiment. The number of cFos+ and eYFP+ cells in the DG region was quantified using an automated ImageJ pipeline that carried out iterative thresholding followed by exclusion of non-circular objects (https://mcib3d.frama.io/3d-suite-imagej/plugins/Segmentation/3D-Iterative-Segmentation/). In order to quantify the number of overlapping cFos+ and eYFP+ cells, an automated algorithm was used to carry out pairwise comparisons between the pixels of each eYFP and cFos cell and the results were filtered to only include overlapping cells of a comparable size (within at least 50% of each-other's size) that were mostly overlapping (85% of smaller object). The accuracy of the automatic counter was verified

against a manually scored dataset created by two experimenters blind to the experimental conditions. Automated counts were used for increased reproducibility. For some comparisons the overlap count was normalized against the size of the Day 1 eYFP+ or the Day 2 cFos+ populations as follows: $\frac{(\boldsymbol{cFos+} \times \boldsymbol{eYFP+})}{eYFP+}$ (Overlap to eYFP ratio) and $\frac{(\boldsymbol{cFos+} \times \boldsymbol{eYFP+})}{cFos+}$ (Overlap to cFos ratio).

## 2.8 Statistical Analysis

Bar graphs are reported as means +/- SEM. Kruskal-Wallis non-parametric tests were used to assess group differences for both cell counts and behavior, and follow-up comparisons made where appropriate using independent T-tests (Tukey's HSD). Repeated measures behavioral comparisons across days but within groups were performed using Wilcoxon signed-rank tests. In cases comparing two groups on the same day, or effects of sex and Half-T route direction, the Mann-Whitney *U*-test was used. Test statistics, groups sizes, and p-values are reported in figure legends. All tests were performed in Matlab using publicly available functions. For all figures, * = $p < 0.05$, ** = $p < 0.01$, *** = $p < 0.001$.

## 2.9 Data Availability

All relevant data supporting the findings of this study are available from the corresponding author upon reasonable request.

# 3. RESULTS

To investigate cells in Dentate Gyrus (DG) associated with spatial navigation memories, we trained mice on a delayed-non-match-to-position (DNMP) task (Fig. 1A). A dox-inducible viral labeling strategy was used to selectively label *c-Fos+* DG cells associated with learning (Fig. 1B). After pre-training and surgical recovery, dox diet was removed from the cage and mice were exposed to a novel T-maze (Context A) in which they performed the DNMP task (Fig. 1C). The mice were returned to dox to prevent off-target labeling and exposed on the following day to another environment. The first group (Full-T) repeated the DNMP behavior in Context A as before. The second group was returned to a version of the maze with one arm permanently blocked (Context B) but otherwise similar with respect to timing delays and sucrose rewards. Mice in this group had visual access to the other side of the maze. The final group was exposed to a novel open field arena without reward contingency (Context C).

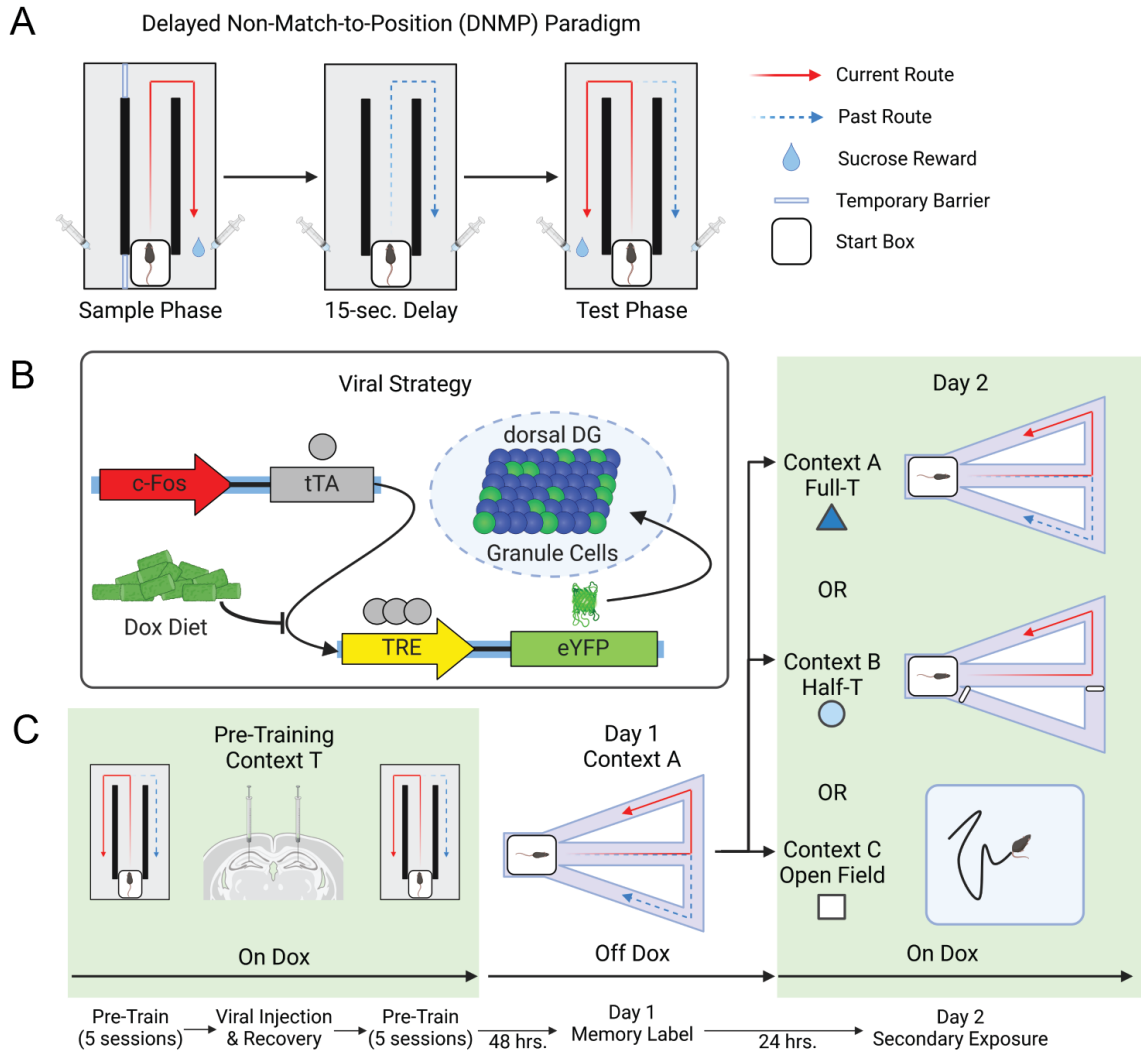


**Figure 1.** Behavioral and viral tagging paradigm used to visualize the spatial engram. **A)** Schematic representation of the delayed-non-match-to-position (DNMP) T-maze task. In the sample phase, an opaque barrier is inserted to force the mouse to traverse one route and receive sucrose reward. After a 15-second start box delay, the mouse must choose to traverse the opposite route to receive a second reward in the test phase.
**B)** Viral constructs AAV9-cFos-tTA and AAV9-TRE-eYFP used in the engram labeling system. Endogenously expressed cFos in transfected Dentate Gyrus cells drives tetracycline-transactivator (tTA) which binds to the tetracycline response element (TRE) and drives expression of eYFP in the absence of doxycycline (Dox).
**C)** Behavioral timeline. Mice (n=18) were pre-trained for 10 sessions, 5 before and 5 after surgical injection of the viral constructs outlined in B. Dox diet was removed from the home cage to open a memory labeling window. Day 1 performance of the DNMP-task in a novel Context A for 20 minutes caused cFos Dentate Gyrus cells to express eYFP. On Day 2 mice were exposed for 20 minutes to the full maze task (Full-T, n=6), the same maze but with one arm blocked (Half-T, n=6), or a novel arena (Open Field, n=6). Brains were collected 90 minutes after the behavioral experience on Day 2.

238

We first examined the size and degree of overlap between DG cell ensembles to determine the degree of representational similarity across days in each group. Immunohistochemical staining revealed two populations, the first from the Day 1 experience (eYFP) and the second from the Day 2 experience (cFos) with partial reactivation (overlap; Fig. 2A-F). Performance of the DNMP T-maze task on Day 1 yielded similar ensemble size across groups as expected and larger ensembles than those on Day 2 in all groups (Fig. 3A). No difference was found in Day 2 ensemble size across groups. Finally, we normalized the number of overlapping cells to the size of the Day 1 population and found a dissociation of reactivation across groups, with the Full-T experiencing highest overlap and Open Field experiencing the least (Fig. 3B). We repeated this analysis with normalization against the Day 2 population size and observed that both the Full-T and Half-T had higher reactivation than the Open Field when compared against the smaller Day 2 population size (Fig. 3C). These results suggest an effect of both novelty and trajectory experience on the recruitment and reactivation of the DG spatial engram ensemble.

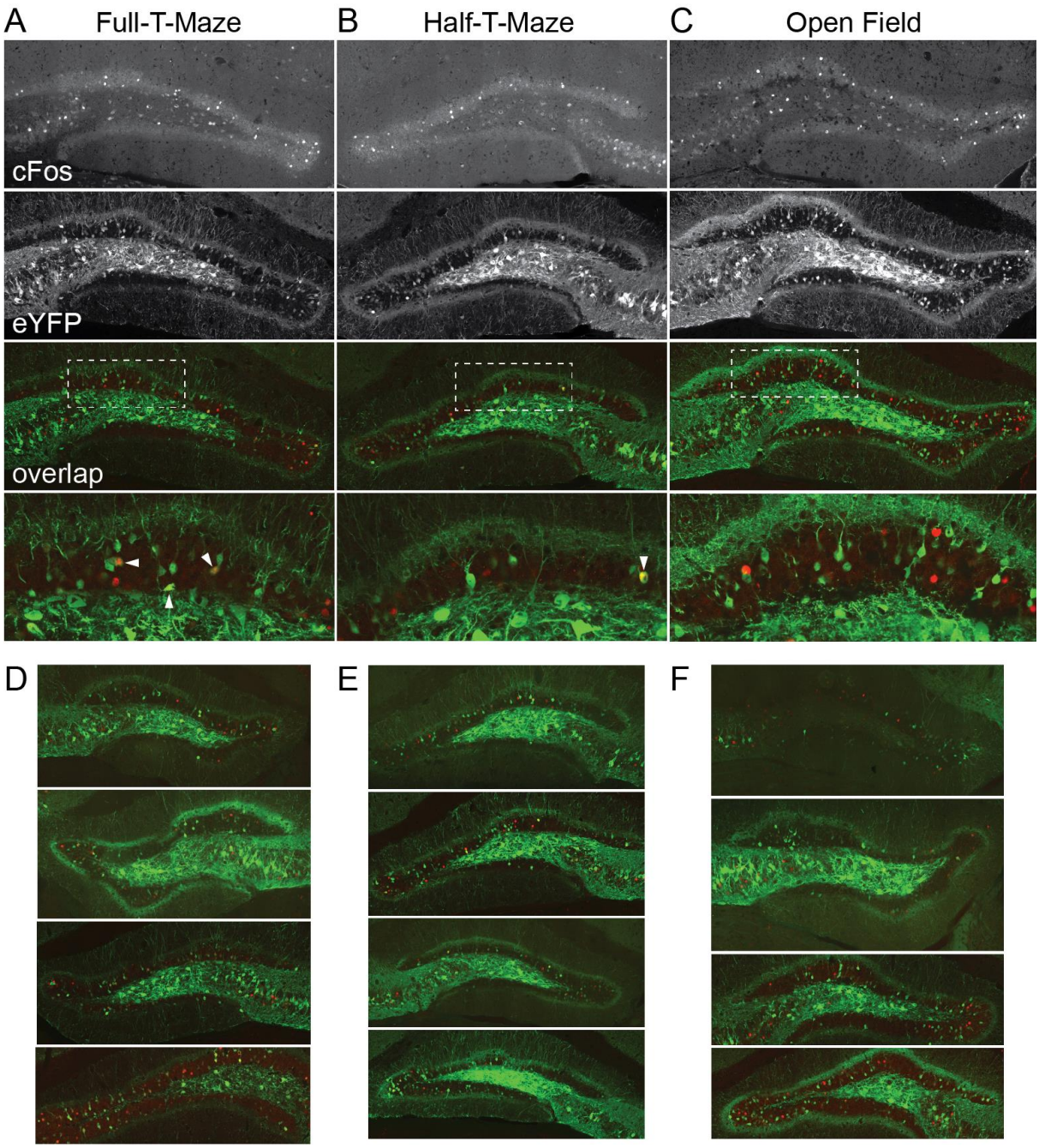


**Figure 2.** Histological staining reveals distinct, partially overlapping spatial engram populations in DG. **A-C)** Representative 60x confocal images of DG from the Full-T, Half-T and Open Field groups. Top row: cFos signal. Upper middle row: eYFP signal. Lower middle row: merge of the above rows (cFos red, eYFP green). Bottom: Zoomed section from the above merge indicated by the white dashed box. White triangles indicate overlap cells active on both days.
**D-F)** Further examples from four different animals per group outlined above in A-C.

254

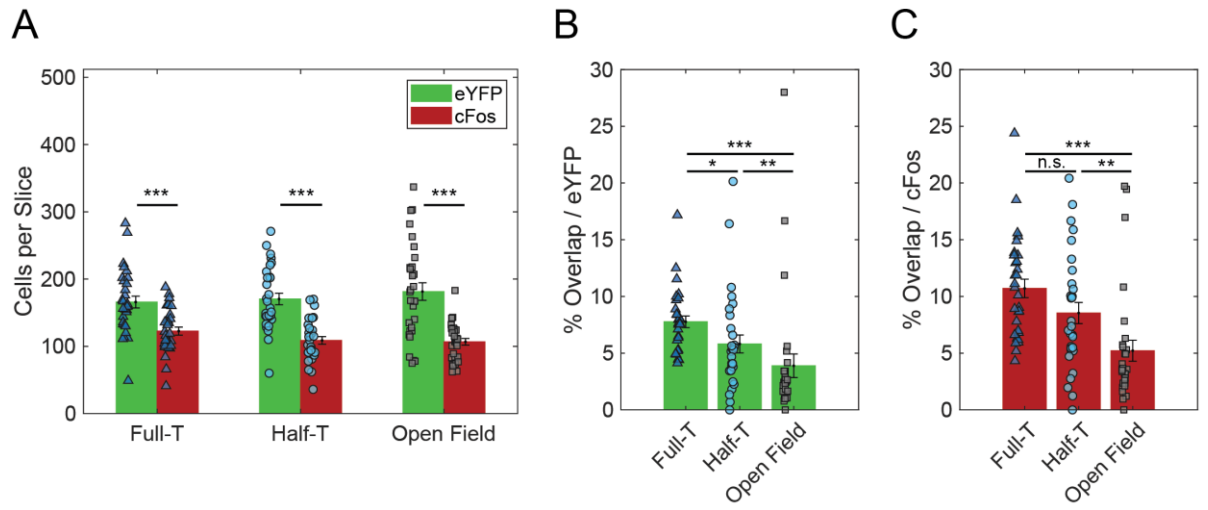


**Figure 3.** DG encodes different routes within a maze using partially non-overlapping populations.
**A)** Day 1 experience in the DNMP task recruited more cells (eYFP) per slice than Day 2 experience (cFos) in all groups (MWU-test; Full-T: $Z = 3.79$, $p < 0.001$; Half-T $Z = 5.06$, $p < 0.001$; Open Field: $Z = 4.41$, $p < 0.001$; n = 30 slices from 6 animals per group). There was no difference in Day 1 ensemble size ($X^2 = 0.59$, $p = 0.74$) or in Day 2 ensemble size ($X^2 = 4.35$, $p = 0.11$) across groups.
**B)** Experience of the Day 2 environments and tasks resulted in differing ensemble reactivation (overlap) between groups when normalized to the Day 1 (eYFP) ensemble size ($X^2 = 30.67$, $p < 0.001$). Posthoc comparisons revealed significant differences between all groups (Tukey's HSD; Full-T vs Half-T: $p = 0.026$; Full-T vs Open Field: $p < 0.001$; Half-T vs Open Field: $p < 0.01$; n = 30 slices from 6 animals per group).
**C)** Same as B but normalized against the Day 2 (cFos) ensemble size ($X^2 = 24.13$, $p < 0.001$). Posthoc comparisons revealed significant differences between the Open Field group and the other groups (Full-T vs Open Field: $p < 0.001$; Half-T vs Open Field: $p < 0.01$) but not between the Full-T and Half-T groups.
Error bars represent +/- SEM. Scatter plots denote individual slices (triangle = Full-T, circle = Half-T, square = Open Field).

To rule out the possibility of confounding effects such as task engagement, laps traversed, and behavioral activity level on engram ensemble recruitment, we analyzed behavior across groups. We found no difference in task accuracy across groups on Day 1, and no change in accuracy across days for the Full-T group (Fig. 4A). These data demonstrate that the mice grasped the task and transferred learning successfully from training Context T to the novel Context A. Next, we examined the number of laps, defined as a trajectory from the start box to the reward then back to the start box, across groups and days. The Half-T group performed significantly fewer laps relative to the Full-T group on Day 2 (Fig. 4B), possibly reflecting a shift to a different behavioral demand (Satvat et al., 2011). For a more general comparison of behavior, we analyzed total distance traveled and average running speed in all groups across days, but found no differences (Fig. 4C,D). These analyses suggest that the degree of engram reactivation is not a result of trajectory length or self-motion cues, but is instead related to behavioral contingencies and experienced trajectories, as hypothesized.

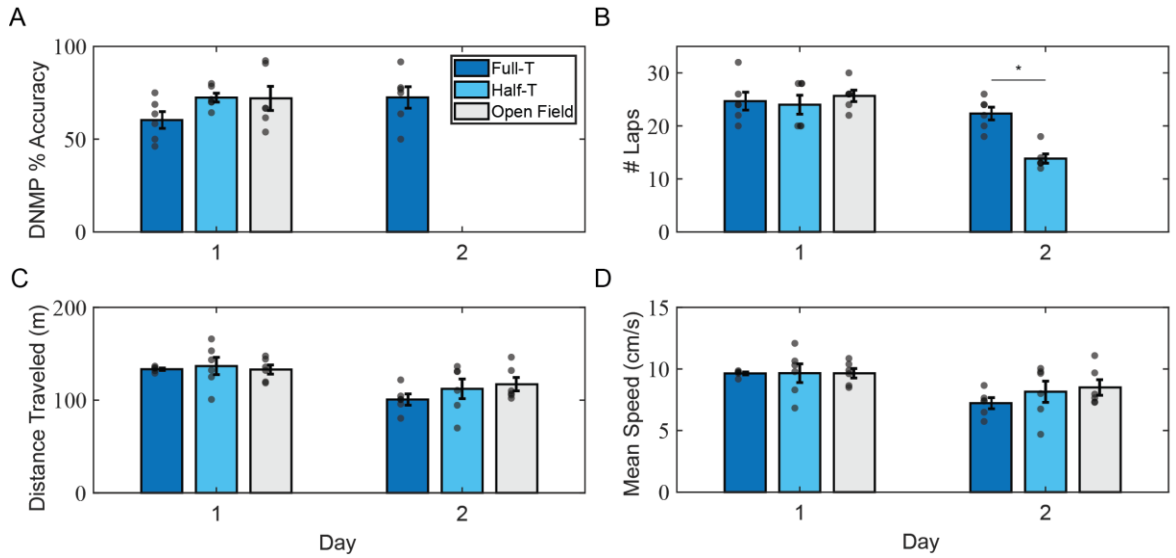


**Figure 4.** DG spatial engram composition relates to experienced trajectories not distance or velocity.
**A)** No differences in DNMP task accuracy were found across groups on Day 1 ($X^2$ = 4.09, p = 0.13) nor did the Full-T group perform differently across days (Wilcoxon signed-rank test, *W* = 4.00, p = 0.22).
**B)** Groups did not run different numbers of laps on Day 1 ($X^2$ = 0.42, p = 0.81) but the Half-T group performed significantly fewer laps relative to the Full-T group on Day 2 (MWU-test, *U* = 45.00, p = 0.013). No difference was found after correction for multiple comparisons across days in the Full-T group (Wilcoxon signed-rank test, *W* = 11.50, p = 1.00) or the Half-T group (*W* = 21.00, p = 0.094).
**C)** The total distance traveled did not differ across groups on Day 1 ($X^2$ = 0.85, p = 0.65) or Day 2 ($X^2$ = 3.40, p = 0.18) nor across days in any group (Wilcoxon signed-rank test; Full-T, *W* = 15.00, p = 0.19; Half-T, *W* = 21.00, p = 0.094; Open Field, *W* = 19.00, p = 0.28).
**D)** The average velocity did not differ across groups on Day 1 ($X^2$ = 0.46, p = 0.80) or Day 2 ($X^2$ = 1.98, p = 0.37) nor across days in any group (Wilcoxon signed-rank test; Full-T, *W* = 15.00, p = 0.19; Half-T, *W* = 21.00, p = 0.094; Open Field, *W* = 17.00, p = 0.66).
Error bars represent +/- SEM. Scatter plots denote individual mice.

Finally, we tested for possible effects of sex and Half-T trajectory direction on spatial engram composition. No difference was found in the ensemble overlap normalized to either Day 1 or Day 2 when comparing male and female mice (Fig. 5A). At the behavioral level, no differences were observed between male and female mice in terms of accuracy, lap number, distance traveled or average velocity on either Day 1 or Day 2 (Fig. 5B). To validate the decision to collapse groups that experienced the left-only or right-only trajectories on Day 2 into a single Half-T group, we performed similar comparisons in these subgroups. The subgroups did not differ in terms of ensemble overlap ratio (Fig. 5C) nor in any of the behavioral metrics of accuracy, laps, distance or speed (Fig. 5D). These results validate the decision to collapse groups by sex and Half-T subgroup, and additionally suggest that male and female mice use similarly sized ensembles in the DG during these task demands.

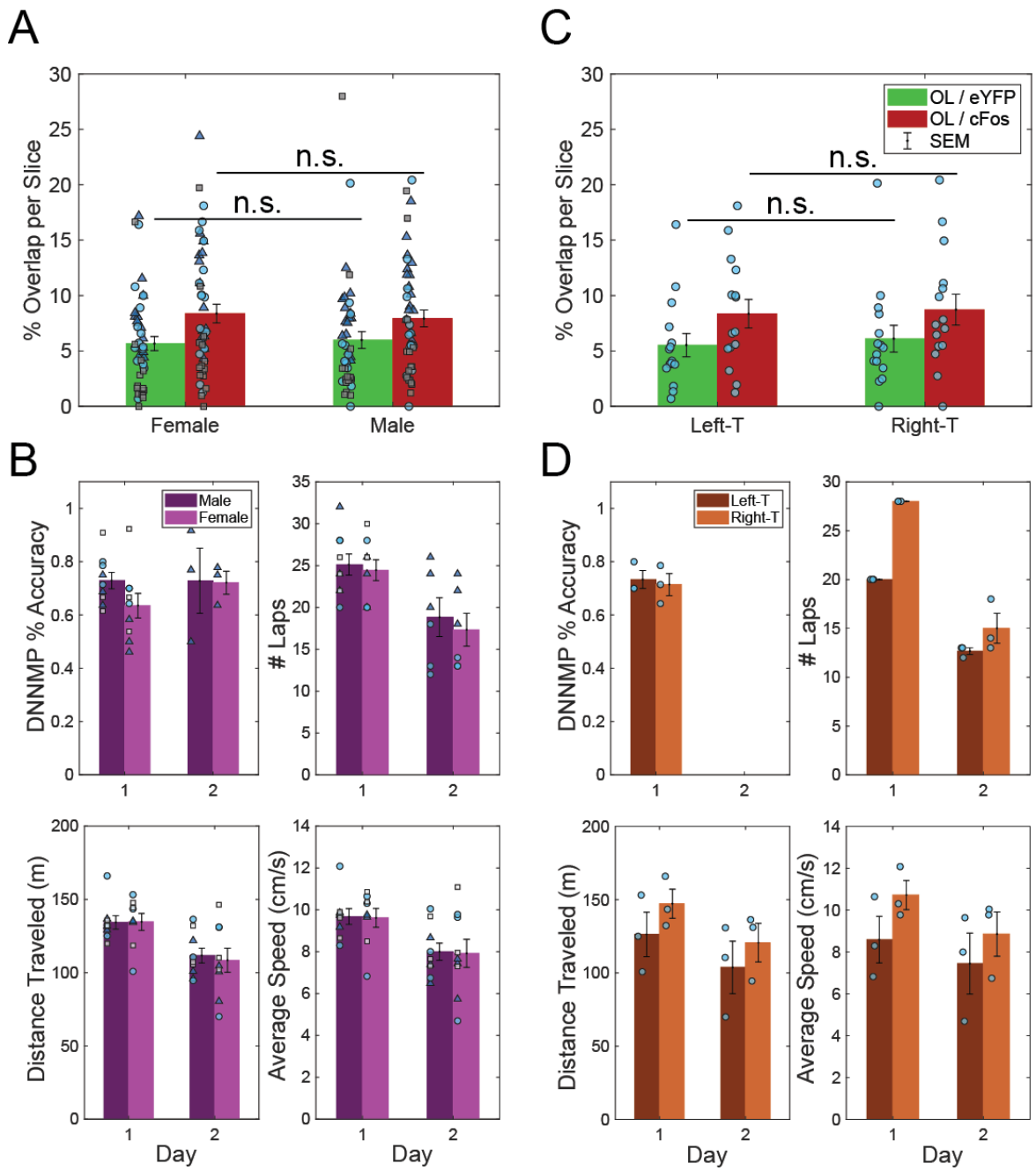


**Figure 5.** Engram composition does not differ across sex or experienced trajectory in the Half-T group.

**A)** The degree of reactivation (overlap cells) did not differ between male (n=45 slices) and female mice (n=45 slices) when normalized to either the Day 1 eYFP population (green; MWU-test, $Z = 0.077$, $p = 0.94$) or Day 2 cFos population (red; $Z = 0.26$, $p = 0.80$). 9 mice of each sex were used.

**B)** No sex differences were found for Day 1 behaviors (MWU-test; Accuracy, $U = 104.50$, $p = 0.098$; Laps, $U = 89.00$, $p = 0.76$; Distance, $U = 73.00$, $p = 0.48$; Velocity, $U = 75.00$, $p = 0.60$) or for Day 2 behaviors (Accuracy, $U = 11.00$, $p = 1.00$; Laps, $U = 41.00$, $p = 0.78$; Distance, $U = 90.00$, $p = 0.73$; Velocity, $U = 87.00$, $p = 0.93$). *Continued on the following page.*

*Fig. 5. Continued from previous page*
**C)** The degree of reactivation did not differ within the Half-T group for mice that ran the left (n=15 slices) or the right side (n=15 slices) of the T-maze when normalized to either the Day 1 eYFP population (green; MWU-test, Z = 0.50, p = 0.62) or the Day 2 cFos population (red; Z = 0.21, p = 0.84). 3 mice per Half-T subgroup.
**D)** No behavioral differences were found between mice in the Half-T group running the Left trajectory (n=3) or the Right trajectory (n=3) on either Day 1 (MWU-test; Accuracy, *U* = 11.00, p = 1.00; Laps, *U* = 6.00, p = 0.10; Distance, *U* = 8.00, p = 0.40; Velocity, *U* = 8.00, p = 0.40) or Day 2 (Laps, *U* = 7.00, p = 0.30; Distance, *U* = 8.00, p = 0.40; Velocity, *U* = 8.00, p = 0.40).
Error bars represent +/- SEM. Scatter plots denote individual mice (triangle = Full-T, circle = Half-T, square = Open Field).

# 4. DISCUSSION

We trained mice to run a delayed-non-match-to-position (DNMP) T-maze task and used an activity-dependent viral labeling strategy to visualize cell populations from different days associated with goal-directed navigation, i.e. spatial engrams. We found that repeated experience with the same two-route spatial working memory task and physical location across days yielded the highest degree of engram similarity (Full-T; Fig. 3B). Conversely, mice performing a navigation task in the same physical space but with only one route (Half-T) showed less reactivation of the original population but higher reactivation than mice exposed to a novel open field (3C). In addition, the size of the recruited ensemble differed based on both experience level and working memory demand such that the Day 2 population was smaller than the Day 1 population in all groups, despite the Open Field mice experiencing two novel contexts in a row (Fig. 3A). Together, these results are consistent with past studies implicating the DG in spatial memory processing (McNaughton et al., 1989; Emerich & Walsh, 1990; Xavier et al., 1999), including T-maze tasks with long delays (Emerich & Walsh, 1989; Costa et al., 2005) and build on previous applications of immediate early genes (IEGs) to study the overlap of populations involved in hippocampal spatial and task-specific memories (Guzowski et al., 1999; Satvat et al., 2011).

## 4.1 Spatial vs fear engrams

We set out to test whether methodologies typically used to label contextual memories in dorsal DG could be used to probe aspects of navigational memory for specific routes within a larger environment. Previous studies of memory ensemble, or engram, composition have largely focused on the formation and reactivation of contextual memories with strong emotional valence, in particular fear (Liu et al., 2012b; Ramirez et al., 2013; Redondo et al., 2014; Chen et al., 2019; Sun et al., 2020). However, physiological recordings from DG during navigation have revealed spatial preferences of DG granule and mossy cells (Jung & McNaughton, 1993; Leutgeb et al., 2007; Neunuebel & Knierim, 2012, 2014; GoodSmith et al., 2017, 2022) which may be stable across days

(Hainmueller & Bartos, 2018; Cholvin et al., 2021). While IEGs have been used to examine cell population reactivation across or within open field navigation contexts (Guzowski et al., 1999), this approach could not distinguish an engram ensemble coding for contextual cues (e.g. odor, distal visual landmarks, etc.) from one encoding specific navigational trajectories (e.g. serially activated place fields). In our study, the Half-T group had lower ensemble reactivation than the Full-T group, but higher reactivation than the Open Field group (Fig. 3B). Based on this finding and previous evidence for spatial specificity in DG granule cells, we hypothesize that different routes are encoded by different spatial engram populations. However, some contribution of pattern separation as a result of differences in behavioral demand between a spatial working memory task (Full-T) and a sensory-guided navigation task with similar delays and rewards (Half-T) is possible (Satvat et al., 2011). Overlap observed in the open field group is likely attributable to chance and some distal global room context cues which were identical to those for the other groups.

## 4.2 Size of the Engram Ensemble

cFos IEG expression arises from neural activity and leads to various plasticity-related changes within a cell (Labiner et al., 1993). Novelty is an important factor for inducing plasticity in the hippocampus, including DG (McNaughton & Morris, 1987; Kitchigina et al., 1997; Straube, Korz, & Frey, 2003; Straube, Korz, Balschun, et al., 2003; Davis et al., 2004). We found increased size of the Day 1 ensemble relative to the Day 2 ensemble in all cases, consistent with a novelty effect in the Full-T and Half-T groups (Fig. 3A). However, the Open Field group underwent a novel context exposure on each day and still exhibited a smaller ensemble on Day 2, which suggests an impact not only of novelty but also task in this study. The open field free-exploration task has no route constraints by design, and these mice were just as active as their Full-T and Half-T counterparts (Fig. 4C,D). Thus, the navigational memory demand and reward contingencies likely play a role in DG ensemble recruitment in addition to novelty alone (Costa et al., 2005)

## 4.3 Composition of sub-ensembles for pattern separation

Studies of dynamic hippocampal activity shed light on the proportion of engram cells reactivated across days. One recent study used calcium imaging to examine the dynamics of DG granule cells during learning of a sensory-guided T-maze task, and found that place field stability correlated with behavioral performance (Shen et al., 2021). Alongside other DG imaging studies showing high cross-day similarity of spatial representations in well-trained animals (Hainmueller & Bartos, 2018; Cholvin et al., 2021), we can speculate about the mechanisms underlying the observed 7.8% reactivation in the Full-T group relative to Day 1. While the mice generalized learning well (Fig. 4A), the Day 1 ensemble was recruited by experience of a maze with novel geometry, odor,

texture, and position within the testing room, yielding a competition between pattern completion and pattern separation respectively (Nakashiba et al., 2012; Santoro, 2013). Follow up studies could compare ensembles tagged in the training context, or pre-trained versus naïve mice, to disambiguate these competing factors on spatial engram composition.

One question concerns whether the DG contains cells with context-modulated spatial tuning, i.e. splitter cells, like those observed in CA1 (Wood et al., 2000; Ferbinteanu & Shapiro, 2003; Griffin et al., 2007; Kinsky et al., 2020). Splitter cells can emerge early in learning and may be modulated by the turn direction, task phase, or both on the DNMP T-maze task (Levy et al., 2021). DG place fields remap based on task engagement, hinting at the flexibility of DG cells within the same physical location (Shen et al., 2021). Interestingly, CA1 splitter cells appear more stable than classic place fields across days, which might help to explain increased overlap observed in the Full-T group relative to the Half-T group which did not experience context-modulation on Day 2 (Fig 3B; Kinsky et al., 2020). However, care must be taken because there was not a statistically difference in overlap between the Full-T and Half-T groups when normalized against the Day 2 ensemble size (Fig. 3C), despite the Half-T mean overlap being lower than the Full-T mean. One explanation is that a smaller, more efficient ensemble is recruited by familiar Day 2 experience (Fig. 3A), and route-specific place cells in the Half-T group make up a large enough population to be indistinguishable from the Day 2 Full-T ensemble composed of place cells from both routes and potential splitters. We cannot rule out the possibility that the DG exhibits classic splitter dynamics with sufficient exposure to a particular navigation route. Splitter cells may indeed serve an additional pattern separation function in DG for this task by discriminating otherwise similar stem trajectories and improving pattern completion of orthogonal sub-ensembles coding for separate reward arm routes (O'Reilly & McClelland, 1994; Wood et al., 2000; Ferbinteanu & Shapiro, 2003; Hasselmo & Eichenbaum, 2005; Nakashiba et al., 2012; Neunuebel & Knierim, 2012, 2014; GoodSmith et al., 2017, 2019; Senzai & Buzsáki, 2017; Hainmueller & Bartos, 2018).

### 4.4 Conclusion

We tested whether experience with specific navigation routes could be dissected in the dentate gyrus using engram tagging and visualization strategies. We found that repeated experience of a two-route maze task across days recruited a more similar ensemble than exposure to a novel open field arena or exposure to a one-route task within the same T-maze environment. The experimental design offers a means to study aspects of spatial navigation using traditional engram tagging techniques. Additionally, our results suggest the dentate gyrus performs its role in pattern separation and spatial navigation by the activation of partially non-overlapping sub-ensembles for different routes in a larger context.

## Acknowledgments

We thank the Hasselmo and Ramirez labs for thoughtful feedback and commentary on the work.

This work was supported by the National Institutes of Health [grant numbers: R01 MH052090, MH060013, MH120073, HD101402-02; and DP5 OD023106-01], and the Office of Naval Research [grant numbers: MURI N00014-16-1-2832, N00014-19-1-2571; and DURIP N00014-17-1-2304].

## Author Contributions

Conceptualization, L.K.W., S.R., and M.E.H.; Methodology, L.K.W. and I.K.; Investigation, L.K.W. and I.K.; Writing – Original Draft, L.K.W., I.K.; Writing – Review & Editing, L.K.W., I.K., S.R., and M.E.H.; Funding Acquisition, M.E.H. and S.R.; Formal Analysis, L.K.W. and I.K.; Visualization, L.K.W.; Supervision, M.E.H. and S.R.

## Declaration of Competing Interest

The authors declare no competing interests.

## References


Chen, B. K., Murawski, N. J., Cincotta, C., McKissick, O., Finkelstein, A., Hamidi, A. B., Merfeld, E., Doucette, E., Grella, S. L., Shpokayte, M., Zaki, Y., Fortin, A., & Ramirez, S. (2019). Artificially Enhancing and Suppressing Hippocampus-Mediated Memories. *Current Biology*, *29*(11), 1885-1894.e4. https://doi.org/10.1016/j.cub.2019.04.065

Cholvin, T., Hainmueller, T., & Bartos, M. (2021). The hippocampus converts dynamic entorhinal inputs into stable spatial maps. *Neuron*, *109*(19), 3135-3148.e7. https://doi.org/10.1016/j.neuron.2021.09.019

Costa, V. C. I., Bueno, J. L. O., & Xavier, G. F. (2005). Dentate gyrus-selective colchicine lesion and performance in temporal and spatial tasks. *Behavioural Brain Research*, *160*(2), 286–303. https://doi.org/10.1016/j.bbr.2004.12.011

Davis, C. D., Jones, F. L., & Derrick, B. E. (2004). Novel Environments Enhance the Induction and Maintenance of Long-Term Potentiation in the Dentate Gyrus. *The Journal of Neuroscience*, *24*(29), 6497–6506. https://doi.org/10.1523/JNEUROSCI.4970-03.2004

Denny, C. A., Kheirbek, M. A., Alba, E. L., Tanaka, K. F., Brachman, R. A., Laughman, K. B., Tomm, N. K., Turi, G. F., Losonczy, A., & Hen, R. (2014). Hippocampal Memory Traces Are Differentially Modulated by Experience, Time, and Adult Neurogenesis. *Neuron*, *83*(1), 189–201. https://doi.org/10.1016/j.neuron.2014.05.018

Emerich, D. F., & Walsh, T. J. (1989). Selective working memory impairments following intradentate injection of colchicine: Attenuation of the behavioral but not the neuropathological effects by gangliosides GM1 and AGF2. *Physiology & Behavior*, *45*(1), 93–101. https://doi.org/10.1016/0031-9384(89)90170-4

Emerich, D. F., & Walsh, T. J. (1990). Cholinergic cell loss and cognitive impairments following intraventricular or intradentate injection of colchicine. *Brain Research*, *517*(1–2), 157–167. https://doi.org/10.1016/0006-8993(90)91021-8

Ferbinteanu, J., & Shapiro, M. L. (2003). Prospective and Retrospective Memory Coding in the Hippocampus. *Neuron*, *40*(6), 1227–1239. https://doi.org/10.1016/S0896-6273(03)00752-9

GoodSmith, D., Chen, X., Wang, C., Kim, S. H., Song, H., Burgalossi, A., Christian, K. M., & Knierim, J. J. (2017). Spatial Representations of Granule Cells and Mossy Cells of the Dentate Gyrus. *Neuron*, *93*(3), 677-690.e5. https://doi.org/10.1016/j.neuron.2016.12.026

GoodSmith, D., Kim, S. H., Puliyadi, V., Ming, G., Song, H., Knierim, J. J., & Christian, K. M. (2022). Flexible encoding of objects and space in single cells of the dentate gyrus. *Current Biology*, *0*(0). https://doi.org/10.1016/j.cub.2022.01.023

GoodSmith, D., Lee, H., Neunuebel, J. P., Song, H., & Knierim, J. J. (2019). Dentate Gyrus Mossy Cells Share a Role in Pattern Separation with Dentate Granule Cells and Proximal CA3 Pyramidal Cells. *The Journal of Neuroscience*, *39*(48), 9570–9584. https://doi.org/10.1523/JNEUROSCI.0940-19.2019

Griffin, A. L., Eichenbaum, H., & Hasselmo, M. E. (2007). Spatial Representations of Hippocampal CA1 Neurons Are Modulated by Behavioral Context in a Hippocampus-Dependent

Memory Task. *Journal of Neuroscience*, *27*(9), 2416–2423. https://doi.org/10.1523/JNEUROSCI.4083-06.2007

Guzowski, J. F., McNaughton, B. L., Barnes, C. A., & Worley, P. F. (1999). Environment-specific expression of the immediate-early gene Arc in hippocampal neuronal ensembles. *Nature Neuroscience*, *2*(12), 1120–1124. https://doi.org/10.1038/16046

Hainmueller, T., & Bartos, M. (2018). Parallel emergence of stable and dynamic memory engrams in the hippocampus. *Nature*, *558*(7709), 292–296. https://doi.org/10.1038/s41586-018-0191-2

Hasselmo, M. E., & Eichenbaum, H. (2005). Hippocampal mechanisms for the context-dependent retrieval of episodes. *Neural Networks*, *18*(9), 1172–1190. https://doi.org/10.1016/j.neunet.2005.08.007

Hasselmo, M. E., & Wyble, B. P. (1997). Free recall and recognition in a network model of the hippocampus: Simulating effects of scopolamine on human memory function. *Behavioural Brain Research*, *89*(1–2), 1–34. https://doi.org/10.1016/S0166-4328(97)00048-X

Jung, M. W., & McNaughton, B. L. (1993). Spatial selectivity of unit activity in the hippocampal granular layer. *Hippocampus*, *3*(2), 165–182. https://doi.org/10.1002/hipo.450030209

Kinsky, N. R., Mau, W., Sullivan, D. W., Levy, S. J., Ruesch, E. A., & Hasselmo, M. E. (2020). Trajectory-modulated hippocampal neurons persist throughout memory-guided navigation. *Nature Communications*, *11*, 2443. https://doi.org/10.1038/s41467-020-16226-4

Kitamura, T., Ogawa, S. K., Roy, D. S., Okuyama, T., Morrissey, M. D., Smith, L. M., Redondo, R. L., & Tonegawa, S. (2017). Engrams and circuits crucial for systems consolidation of a memory. *Science*, *356*(6333), 73–78. https://doi.org/10.1126/science.aam6808

Kitchigina, V., Vankov, A., Harley, C., & Sara, S. J. (1997). Novelty-elicited, Noradrenaline-dependent Enhancement of Excitability in the Dentate Gyrus. *European Journal of Neuroscience*, *9*(1), 41–47. https://doi.org/10.1111/j.1460-9568.1997.tb01351.x

Labiner, D., Butler, L., Cao, Z., Hosford, D., Shin, C., & McNamara, J. (1993). Induction of c-fos mRNA by kindled seizures: Complex relationship with neuronal burst firing. *The Journal of Neuroscience*, *13*(2), 744–751. https://doi.org/10.1523/JNEUROSCI.13-02-00744.1993

Leutgeb, J. K., Leutgeb, S., Moser, M.-B., & Moser, E. I. (2007). Pattern Separation in the Dentate Gyrus and CA3 of the Hippocampus. *Science*, *315*(5814), 961–966. https://doi.org/10.1126/science.1135801

Levy, S. J., Kinsky, N. R., Mau, W., Sullivan, D. W., & Hasselmo, M. E. (2021). Hippocampal spatial memory representations in mice are heterogeneously stable. *Hippocampus*, *31*(3), 244–260. https://doi.org/10.1002/hipo.23272

Liu, X., Ramirez, S., Pang, P. T., Puryear, C. B., Govindarajan, A., Deisseroth, K., & Tonegawa, S. (2012a). Optogenetic stimulation of a hippocampal engram activates fear memory recall. *Nature*, *484*(7394), 381–385. https://doi.org/10.1038/nature11028

Marr, D. (1971). Simple memory: A theory for archicortex. *Philosophical Transactions of the Royal Society of London. B, Biological Sciences*, *262*(841), 23–81. https://doi.org/10.1098/rstb.1971.0078

Mathis, A., Mamidanna, P., Cury, K. M., Abe, T., Murthy, V. N., Mathis, M. W., & Bethge, M. (2018). DeepLabCut: Markerless pose estimation of user-defined body parts with deep learning. *Nature Neuroscience*, *21*(9), 1281–1289. https://doi.org/10.1038/s41593-018-0209-y

McLamb, R. L., Mundy, W. R., & Tilson, H. A. (1988). Intradentate colchicine disrupts the acquisition and performance of a working memory task in the radial arm maze. *Neurotoxicology*, *9*(3), 521–528.

McNaughton, B. L., Barnes, C. A., Meltzer, J., & Sutherland, R. J. (1989). Hippocampal granule cells are necessary for normal spatial learning but not for spatially-selective pyramidal cell discharge. *Experimental Brain Research*, *76*(3), 485–496. https://doi.org/10.1007/BF00248904

McNaughton, B. L., & Morris, R. G. M. (1987). Hippocampal synaptic enhancement and information storage within a distributed memory system. *Trends in Neurosciences*, *10*(10), 408–415. https://doi.org/10.1016/0166-2236(87)90011-7

Nakashiba, T., Cushman, J. D., Pelkey, K. A., Renaudineau, S., Buhl, D. L., McHugh, T. J., Barrera, V. R., Chittajallu, R., Iwamoto, K. S., McBain, C. J., Fanselow, M. S., & Tonegawa, S. (2012). Young Dentate Granule Cells Mediate Pattern Separation whereas Old Granule Cells Contribute to Pattern Completion. *Cell*, *149*(1), 188–201. https://doi.org/10.1016/j.cell.2012.01.046

Nanry, K. P., Mundy, W. R., & Tilson, H. A. (1989). Colchicine-induced alterations of reference memory in rats: Role of spatial versus non-spatial task components. *Behavioural Brain Research*, *35*(1), 45–53. https://doi.org/10.1016/S0166-4328(89)80007-5

Neunuebel, J. P., & Knierim, J. J. (2012). Spatial Firing Correlates of Physiologically Distinct Cell Types of the Rat Dentate Gyrus. *Journal of Neuroscience*, *32*(11), 3848–3858. https://doi.org/10.1523/jneurosci.6038-11.2012

Neunuebel, J. P., & Knierim, J. J. (2014). CA3 Retrieves Coherent Representations from Degraded Input: Direct Evidence for CA3 Pattern Completion and Dentate Gyrus Pattern Separation. *Neuron*, *81*(2), 416–427. https://doi.org/10.1016/j.neuron.2013.11.017

O'Keefe, J., & Dostrovsky, J. (1971). The hippocampus as a spatial map. Preliminary evidence from unit activity in the freely-moving rat. *Brain Research*, *34*(1), 171–175. https://doi.org/10.1016/0006-8993(71)90358-1

O'Reilly, R. C., & McClelland, J. L. (1994). Hippocampal conjunctive encoding, storage, and recall: Avoiding a trade-off. *Hippocampus*, *4*(6), 661–682. https://doi.org/10.1002/hipo.450040605

Ramirez, S., Liu, X., Lin, P.-A., Suh, J., Pignatelli, M., Redondo, R. L., Ryan, T. J., & Tonegawa, S. (2013). Creating a False Memory in the Hippocampus. *Science*, *341*(6144), 387–391. https://doi.org/10.1126/science.1239073

Redondo, R. L., Kim, J., Arons, A. L., Ramirez, S., Liu, X., & Tonegawa, S. (2014). Bidirectional switch of the valence associated with a hippocampal contextual memory engram. *Nature*, *513*(7518), 426–430. https://doi.org/10.1038/nature13725

Reijmers, L. G., Perkins, B. L., Matsuo, N., & Mayford, M. (2007). Localization of a Stable Neural Correlate of Associative Memory. *Science*, *317*(5842), 1230–1233. https://doi.org/10.1126/science.1143839

Roy, D. S., Arons, A., Mitchell, T. I., Pignatelli, M., Ryan, T. J., & Tonegawa, S. (2016). Memory retrieval by activating engram cells in mouse models of early Alzheimer's disease. *Nature*, *531*(7595), 508–512. https://doi.org/10.1038/nature17172

Santoro, A. (2013). Reassessing pattern separation in the dentate gyrus. *Frontiers in Behavioral Neuroscience*, *7*. https://doi.org/10.3389/fnbeh.2013.00096

Sasaki, T., Piatti, V. C., Hwaun, E., Ahmadi, S., Lisman, J. E., Leutgeb, S., & Leutgeb, J. K. (2018). Dentate network activity is necessary for spatial working memory by supporting CA3 sharp-wave ripple generation and prospective firing of CA3 neurons. *Nature Neuroscience*, *21*(2), 258–269. https://doi.org/10.1038/s41593-017-0061-5

Satvat, E., Schmidt, B., Argraves, M., Marrone, D. F., & Markus, E. J. (2011). Changes in Task Demands Alter the Pattern of zif268 Expression in the Dentate Gyrus. *The Journal of Neuroscience*, *31*(19), 7163–7167. https://doi.org/10.1523/JNEUROSCI.0094-11.2011

Senzai, Y., & Buzsáki, G. (2017). Physiological properties and behavioral correlates of hippocampal granule cells and mossy cells. *Neuron*, *93*(3), 691-704.e5. https://doi.org/10.1016/j.neuron.2016.12.011

Shen, J., Yao, P.-T., Ge, S., & Xiong, Q. (2021). Dentate granule cells encode auditory decisions after reinforcement learning in rats. *Scientific Reports*, *11*(1), 14360. https://doi.org/10.1038/s41598-021-93721-8

Straube, T., Korz, V., Balschun, D., & Uta Frey, J. (2003). Requirement of β-adrenergic receptor activation and protein synthesis for LTP-reinforcement by novelty in rat dentate gyrus. *The Journal of Physiology*, *552*(Pt 3), 953–960. https://doi.org/10.1113/jphysiol.2003.049452

Straube, T., Korz, V., & Frey, J. U. (2003). Bidirectional modulation of long-term potentiation by novelty-exploration in rat dentate gyrus. *Neuroscience Letters*, *344*(1), 5–8. https://doi.org/10.1016/S0304-3940(03)00349-5

Sun, X., Bernstein, M. J., Meng, M., Rao, S., Sørensen, A. T., Yao, L., Zhang, X., Anikeeva, P. O., & Lin, Y. (2020). Functionally Distinct Neuronal Ensembles within the Memory Engram. *Cell*, *181*(2), 410-423.e17. https://doi.org/10.1016/j.cell.2020.02.055

Treves, A., & Rolls, E. T. (1994). Computational analysis of the role of the hippocampus in memory. *Hippocampus*, *4*(3), 374–391. https://doi.org/10.1002/hipo.450040319

Wood, E. R., Dudchenko, P. A., Robitsek, R. J., & Eichenbaum, H. (2000). Hippocampal Neurons Encode Information about Different Types of Memory Episodes Occurring in the Same Location. *Neuron*, *27*(3), 623–633. https://doi.org/10.1016/S0896-6273(00)00071-4

Xavier, G. F., & Costa, V. C. I. (2009). Dentate gyrus and spatial behaviour. *Progress in Neuro-Psychopharmacology and Biological Psychiatry*, *33*(5), 762–773. https://doi.org/10.1016/j.pnpbp.2009.03.036

Xavier, G. F., Oliveira-Filho, F. J. B., & Santos, A. M. G. (1999). Dentate gyrus-selective colchicine lesion and disruption of performance in spatial tasks: Difficulties in “place strategy” because of a lack of flexibility in the use of environmental cues? *Hippocampus*, *9*(6), 668–681. https://doi.org/10.1002/(SICI)1098-1063(1999)9:6<668::AID-HIPO8>3.0.CO;2-9